

## REVIEW

# Three-dimensional cancer models mimic cell–matrix interactions in the tumour microenvironment

David Herrmann, James R.W.Conway, Claire Vennin, Astrid Magenau, William E.Hughes<sup>1</sup>, Jennifer P.Morton<sup>2</sup> and Paul Timpson\*

Cancer Division, Garvan Institute of Medical Research, The Kinghorn Cancer Centre, St. Vincent's Clinical School, Faculty of Medicine, University of New South Wales, NSW 2010, Sydney, Australia, <sup>1</sup>Diabetes and Obesity Division, Garvan Institute of Medical Research, St. Vincent's Clinical School, Faculty of Medicine, University of New South Wales, NSW 2010, Sydney, Australia and <sup>2</sup>The Beatson Institute for Cancer Research, Garscube Estate, Glasgow G61 1BD, UK

\*To whom correspondence should be addressed. Tel: +61 2 9355 5821;  
Fax: +61 2 9355 5869;  
Email: [p.timpson@garvan.org.au](mailto:p.timpson@garvan.org.au)

Basic *in vitro* systems can be used to model and assess complex diseases, such as cancer. Recent advances in this field include the incorporation of multiple cell types and extracellular matrix proteins into three-dimensional (3D) models to recapitulate the structure, organization and functionality of live tissue *in situ*. Cells within such a 3D environment behave very differently from cells on two-dimensional (2D) substrates, as cell–matrix interactions trigger signalling pathways and cellular responses in 3D, which may not be observed in 2D. Thus, the use of 3D systems can be advantageous for the assessment of disease progression over 2D set-ups alone. Here, we highlight the current advantages and challenges of employing 3D systems in the study of cancer and provide an overview to guide the appropriate use of distinct models in cancer research.

## Introduction

Three-dimensional (3D) systems stimulate a spectrum of autocrine, paracrine and cell type-specific behaviours recapitulating vital aspects of cancer progression *in vivo*, which cannot always be simulated in two-dimensional (2D) systems. Here, we outline the benefits and potential caveats of both 2D and 3D *in vitro* systems in faithfully modelling cancer progression and therapeutic intervention. A brief overview of the 3D systems discussed is given in Table I and Figure 1.

## 3D *in vitro* systems can mimic aspects of *in vivo* cell biology

Cancer cell migration and invasion is a 3D process involving cell–cell and cell–matrix interactions, which can be difficult to approximate in conventional 2D cell culture. Indeed, several protrusions and cellular structures found *in vitro* within a 3D environment are also emerging in an *in vivo* context. For example, RhoA-dependent protrusions at the leading edge of pancreatic cancer cells were initially detected *in vitro* within cells invading into an organotypic matrix at depth, but not in 2D cultures (1). These have now been found to exist *in vivo*, and, moreover, can be specifically targeted by anti-metastatic therapy (1,2). Furthermore, the formation of actin-rich podosomes and invadopodia on migrating and invading cells has been observed in 3D environments and in *in vivo* systems (3–9). Additionally, debate has emerged surrounding the presence and composition of focal adhesions within 3D *in vitro* models (10–12). Classical focal adhesion

components, such as paxillin and vinculin, are required for efficient cell migration within 2D and 3D *in vitro* systems (10); however, their distribution and dynamics can differ significantly across both systems (13,14). Interestingly, a recent description of paxillin and vinculin-containing aggregates as potential components of focal adhesions *in vivo* was comparable with similar aggregates in cells within 3D matrices, based on their localization at the cell–matrix interface (15), thus highlighting the utility of 3D systems in modelling cancer behaviour in live tissue.

Although 3D *in vitro* models are becoming increasingly more faithful to the *in vivo* situation, it is important to note that 3D systems may not provide an accurate representation of all cell behaviours *in vivo*. Indeed, recent work has highlighted that cells interact in a range of dimensions *in vivo* (i.e. 1D/3D and 2D/3D) (16). 1D migration describes cell movement within a fibrillar network, in which cells attach to a single fibre, whereas in 1D/3D migration the cells are in contact with several fibres (16,17). 2D migration involves the movement of cells across planar structures, such as basement membranes, which *in vivo* are typically surrounded by additional substrates, engaging cells in 2D/3D migration (16,18). Thus, it is important to consider that the diverse aspects of cancer behaviour *in vivo* can best be mimicked by selecting a range of 2D and 3D *in vitro* systems (described in more detail below).

## 3D *in vitro* systems can simulate relevant aspects of cancer and drug response

The accumulating similarities between 3D *in vitro* systems and *in vivo* allow us to model relevant aspects of physiological as well as pathological conditions *in vitro*. One such example is the formation of spheroids when mammary epithelial cells of the MCF10A cell line are embedded in a 3D matrix. MCF10A spheroids are useful for assessing distinct 3D architectural properties, which cannot be accurately replicated in their functional setting by 2D MCF10A cell culture. Such 3D-specific properties include loss of tissue restraint and gain of an invasive phenotype due to changes in cell–cell adhesions and disruption of apicobasal polarity, luminal survival due to anti-apoptotic and pro-proliferative signals, or the capacity to overcome growth arrest due to pro-proliferative signals and alterations in growth factor dependence (19–28). MCF10A spheroids have revealed a spectrum of spatially and temporally regulated oncogenic drivers that are involved in processes only detectable in a 3D context and that can be stratified according to their biological function, e.g. pro-proliferative E6/7 (22) and Gab2 (23,24), anti-apoptotic Bcl-2 family members (20,25,26) and polarity and epithelial disruptors, such as Scribble (27) or mutant p53 (28). Malfunction in these fundamental processes has also been found in human breast cancers and thus 3D models, like spheroids, can be used as a surrogate guide to the molecular basis of defined aspects of malignant disease.

Likewise, cell-derived matrices (CDMs) provide a reciprocal extracellular matrix (ECM)-based feedback to tumour cell signalling and in many cases can surpass cell culture on 2D substrates in that cell–matrix adhesion, motility and proliferation are enhanced in this setting. These observed differences between CDMs and cells grown in 2D may be due to an increase in dimension or the presence of cytokines and growth factors deposited into CDMs, which are lacking in simpler, non-decorated 2D environments. Furthermore, cells cultured on CDMs are morphologically similar to cells *in vivo*, as they form specialized 3D matrix adhesions that are also detected *in vivo* (13,15,29–32). It is therefore not surprising that signalling and target inhibition can differ significantly between 2D and 3D settings. This has been demonstrated in SKBR-3 breast cancer cells, in which the tyrosine kinase receptors HER2 and HER3 heterodimerize in 2D cultures, whereas in 3D SKBR-3 spheroids, HER2 forms homodimers triggering intracellular signalling pathways and responses distinct from those seen in 2D culture (33).

Similarly, increases in drug resistance have been described in CDMs compared with 2D cultures (34). The breast cancer cell line MDA-MB-231 requires a much higher drug dosage to inhibit survival and invasion when cultured in 3D silk fibroin scaffolds compared with

**Abbreviations:** 2D, two-dimensional; 3D, three-dimensional; CDM, cell-derived matrix; ECM, extracellular matrix; TDM, tissue-derived matrix.

**Table I.** *In vitro* systems for cell migration and invasion studies

Spheroids (Figure 1A)	Spheroids are 3D multicellular structures that form in the absence of cell substrate adhesion. They are commonly generated in rotating devices (e.g. spinner flask or rotating wall vessel) (155), through cell injection into 3D ECM (e.g. collagen gels) (156), or on substrates, such as agarose (157), collagen (158) or Matrigel (19). Cells within a spheroid adhere closely to each other and secrete ECM to constitute a more complex structure reminiscent of <i>in vivo</i> tissue organization (155). Cell spheroids can also be obtained within a small volume of cell suspension that is placed on an inverted lid. The droplet sticks to the lid due to surface tension and cells form a spheroid within, as they are not able to adhere to the lid surface above (159). After formation, spheroids can be embedded into hydrogels or other 3D scaffolds to further simulate a 3D environment (133,134,160).
CDMs (Figure 1B)	CDMs were first described in 1989 whereby hyper-confluent fibroblasts produced a mix of ECM components including collagen, proteoglycans, hyaluronic acid and other proteins over a long-term culture. Composition and strength of this matrix can be altered, e.g. through addition of ascorbic acid or growth factors. Cells of interest are then seeded on top of the CDM to observe migration (115,161).
Hydrogels (Figure 1C)	Hydrogels are 3D matrices consisting of hydrophilic polymers, which can be cross-linked physically by cell-driven contraction or chemically by fixation. The properties of the hydrogel can be modified by alterations to pH and temperature during the polymerization process. Selected examples include Matrigel, myogel and collagen I matrices. Matrigel is a mix of ECM proteins derived from secretions of Engelbreth-Holm-Swarm mouse sarcoma cells into which cells of interest are embedded. Major components are laminin, entactin, perlecan and collagen IV (162–164). Furthermore, new matrix extracts are appearing, such as Myogel, which are capable of guiding adipocytic cell differentiation <i>in vitro</i> (165,166). After gelling, cells are embedded into or seeded on top of the matrix and cell migration can be observed in 3D, similar to migration in CDMs. Collagen I is usually isolated from rat tails or calf skin and polymerized to a gel under alkaline conditions. Fibroblasts can be embedded into the collagen gel to contract and cross-link the matrix. After cell seeding, the matrix is transferred onto a metal grid and exposed to an air–liquid interface, which generates a gradient towards which the cells can migrate if they are able to penetrate and invade into the collagen matrix (as shown in Figure 1C) (124,167). Alternatively cells or spheroids can be embedded into the matrix before it has polymerized.
Microfluidic devices (Figure 1D)	Cells are embedded into a network of channels and subjected to continuous flow. This flow provides fresh medium and allows diffusion of nutrients, drugs or chemokines thus generating a constant and directional flow. Furthermore, the flow provides shear stress, which can be combined with variations in channel materials, mechanical properties and matrix abundance to precisely modify the microenvironment in which the cells grow. Microfluidic devices are especially useful for high-throughput analysis or in the form of chemotaxis chambers for the identification of chemokines or genes and mechanisms regulating chemotaxis (104). Cell migration can be readily imaged live (168,169) or cell proliferation and survival assessed by immunofluorescence (170).

2D cultures (35). In addition, 3D spheroids derived from human and mouse pancreatic ductal adenocarcinoma cells show an increase in drug resistance compared with 2D cell cultures, reflecting pancreatic ductal adenocarcinoma chemoresistance *in vivo* (36). Ovarian cancer cells also display an increase in chemoresistance when grown as 3D spheroids, compared with 2D culture (37). The majority of these phenomena can be attributed to differences in cell–matrix pro-survival interactions in 3D systems compared with 2D culture, which are mediated by changes in integrin receptor localization and activation, and intracellular signal transduction (13,38). Indeed, integrin signalling driven by cell–matrix adhesion confers resistance against chemotherapy-induced apoptosis (39), whereas inhibition of integrin signalling in combination with chemotherapy can lead to an improvement in cytotoxic response (40,41).

Although initially simple and thus ideally suited to high-throughput drug-screening approaches, 2D cultures may lack the fidelity to mimic the complexity of a 3D tumour burden. 3D microenvironments confer a multitude of possibilities to avoid or allay drug function to tumour cells. Thus, 3D modelling of cancer can help to unmask such weaknesses and potential resistance mechanisms, which otherwise would only be detected in late drug discovery stages *in vivo*.

### ECM as a key component of 3D *in vitro* systems

Tumours are heterogeneous tissues, which in addition to tumour cells contain tumour-associated cell types, such as fibroblasts, endothelial cells, pericytes or immune cells, as well as a wide variety of ECM components, such as collagen, hyaluronic acid or elastins, and sequestered growth factors and cytokines (42–47). The dual role of this contextual stroma has recently been highlighted, not only for impairing, but also promoting, malignant progression (48–50). The tumour microenvironment can be permissive, supplying cancer cells with important cues during growth and migration, but can also impair growth and metastasis by suppressing cancer cell proliferation or restricting cell motility. In a recent study, the treatment of 45 cancer cell lines grown alone, or in co-culture with stromal cell lines, with 35 anti-cancer drugs, showed that the stroma conferred significant chemoresistance to cancer cells (51). Thus, the stroma presents a drug target as important as the cancer cells themselves. Furthermore, tissue malperfusion and diffusion barriers, such as dense or complex

ECM, can counteract drug delivery into deeper tissues, acting as a barrier, or sink *in vivo*, ultimately decreasing drug efficacy within the target tissue (52–56). Although malperfusion *in vivo* remains a challenging aspect to recapitulate *in vitro*, 3D hydrogels, such as collagen matrices, offer a possibility to mimic and study dense matrix as a potential diffusion barrier (57,58). Despite their lack of complex ECM composition, drug diffusion is demonstrably reduced in these matrices compared with liquid media (58). This has been correlated with an increase in collagen concentration or cross-linking *in vitro* and *in vivo* (57,59,60), while disruption of the collagen network reportedly increases macromolecular diffusion (52). Similarly, the level of desmoplasia and tumour fibrosis in pancreatic cancer has been shown to impair perfusion and drug delivery to tumours (61). Furthermore, 3D matrices were recently used to optimize ECM-targeted therapy for improved anti-metastatic drug delivery *in vivo* (54). Finally, desmoplastic stroma, including ECM components, such as collagen and hyaluronan, not only serves as a diffusion barrier, but also indirectly inhibits drug delivery by compressing blood vessels and thereby enhancing malperfusion (55,56,62). Understanding the complex interactions between cancer cells and their environment is therefore key to successful therapeutic approaches. This is especially true for designing drugs to inhibit invasion and metastasis, from which the majority of cancer mortalities arise. Hence, in the context of a tumour microenvironment, it becomes crucial to investigate other avenues to explore drug delivery, efficiency and clearance, before proceeding to pre-clinical trials in costly and time-consuming *in vivo* systems.

It has been shown that many tumours, such as mammary, pancreatic and squamous cell carcinoma, express a high amount of collagen I in the ECM *in vivo* (46,63–67) and that a progression in collagen density positively correlates with mammary tumour growth and metastasis (68,69). Furthermore, collagen remodelling and cross-linking facilitates invasion (70,71), making collagen an important component in 3D models of cancer cell invasion and metastasis. Invasion into collagen matrices can be enhanced by increasing the number of fibroblasts or adding Matrigel to the collagen, thus generating a more diverse microenvironment and stimulating additional sets of surface receptors and signalling pathways (72,73). For example, exciting results have been obtained by embedding Schwann cells in 3D matrix hydrogels, consisting of collagen, laminin and hyaluronic acid, all of which are

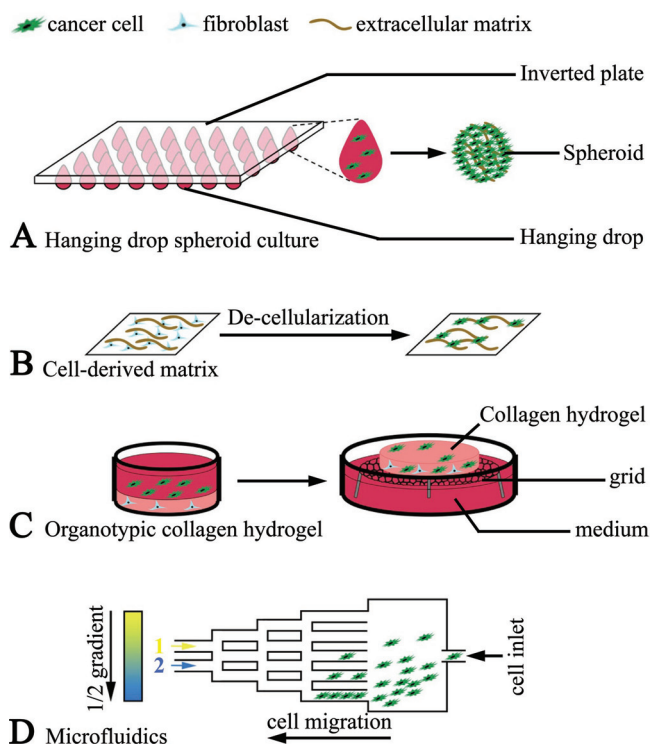


**Fig. 1.** Schematic overview of several 3D *in vitro* systems described in Table I. (A) Spheroids: cells cultured in the absence of adhesion to a substrate, such as in hanging drops attached to an inverted plate, form spheroids characterized by tight cell–cell adhesions and secretion of ECM. (B) CDMs: Hyper-confluent fibroblasts cultured on a coverslip secrete ECM. After de-cellularization of the fibroblasts, cancer cells are seeded on top of the CDM. (C) Hydrogels: fibroblasts embedded into a hydrogel contract the matrix. Cancer cells are seeded on top of the hydrogel and invade into it upon lifting the matrix to an air–liquid interface. (D) Microfluidics: basic principle of a microfluidic device to generate a gradient of two substances (e.g. 1 = medium without chemokine, 2 = medium with chemokine). Single cells are seeded *via* the cell inlet and subjected to this gradient to study cellular responses (e.g. cell migration monitored by live imaging or cell proliferation by immunofluorescence) in correlation to different chemokine or drug concentrations.

expressed in the ECM around Schwann cells *in vivo*. Schwann cells showed an increase in metabolic activity, cell spreading and secretion of neurotrophins in rich 3D matrices consisting of all three components, compared with matrices solely consisting of collagen (74).

In order to further increase microenvironment diversity, a new approach involves the collection of uterine leiomyoma tissue, on which squamous cell carcinoma and breast cancer cells have been seeded, to investigate invasion into a primary tissue environment (75,76). This tissue is much more complex than standard hydrogels, harbouring various cell types, such as endothelial and inflammatory cells, and ECM proteins, such as collagens and laminins. It permits increased invasion depth, affects the mode of invasion and enhances cellular expression of ECM proteins, in contrast to cells seeded onto collagen gels (75). Although the availability and abundance of patient-derived tissue sections may limit large-scale studies, the tissue sections can be stored for long periods between harvesting and cell seeding. The preserved myoma tissue structure may also work as a barrier against drug diffusion, as found in live tissue, making this an attractive system in which to study drug delivery. However, increased tissue fidelity presents two potential caveats in that a given cancer cell type should ideally be matched with respective stromal tissue, e.g. lung cancer cells should be seeded on lung stroma (77). This match may cause distinct cellular and drug responses that do not allow generalized conclusions for other cancer cell types.

Assays addressing the efficiency of a drug to influence cell behaviour *in vivo* may be more meaningful and translational, if they are based on such forms of 3D assessment prior to *in vivo* testing. 3D

investigations with patient-derived primary samples may be suitable as an initial platform for patient stratification studies in personalized therapy to assess potential drug combinations for diverse patient cohorts (78,79).

### Biomechanical properties of the environment influence cell behaviour

Since cells in an *in vivo* scenario are not exposed to a static environment, cell migration and invasion models should include a simulation of mechanical forces that impact on cell behaviour. Extracellular and intracellular mechanical forces (e.g. through matrix stiffness, fluid shear forces or pressure) control *in vivo* cell shape, fate, differentiation and behaviour (80,81). Biomechanical properties of the environment affect cellular processes such as proliferation, apoptosis and migration and also influence malignant progression (55,56,82–84). For example, mammary tumour cells show an increased invasive ability in areas governed by high, compared with low, mechanical stress (85,86), while mechanical deformations and signals from other cell types can stimulate cancer cell invasion (84,87). It is thus crucial to test cells in an environment that simulates *in vivo* mechanical properties. Due to the correlation between tumour progression and increased collagen abundance, stiffness and cross-linking (63,64,68,69), several groups have focussed on analysing cell motility within collagen matrices. It has been demonstrated that fibroblasts overexpressing lysyl oxidase *in vivo* stimulate collagen cross-linking and matrix stiffness (71,88,89). Such stiffened matrices promote cancer cell invasion, whereas inhibition of collagen cross-linking and matrix stiffness reduces tumour progression (69). Stiff matrices enhance cell proliferation and elicit chemoresistance in hepatocellular carcinoma cells (90). Hence, the cytotoxic effects of paclitaxel have been analysed in several cancer cell lines within collagen-coated polyacrylamide wells of varying stiffness (91). It was shown that substrate pliability can influence cytotoxic response and drug resistance, underscoring the necessity to use defined matrix characteristics in screening assays (91). Matrigel, a basement membrane extract which has been used extensively to study invasion, was shown to be significantly less stiff than basement membrane structures *in vivo* (92). Similarly, the elastic modulus of lung CDM is below physiological values, but can be increased by fixation with glutaraldehyde prior to cell seeding (93). Thus, when investigating cancer cell behaviour, it is necessary to know the biomechanical properties of the substrates used, otherwise conclusions cannot accurately be extrapolated to an *in vivo* scenario.

### Modulation of biomechanical ECM properties *in vitro*

Slight alterations in the density of the collagen matrix can result in exquisitely modulated responses of embedded cells (94). For instance, in low-density collagen, breast cancer cells can form polarized structures, whereas in higher density collagen they can proliferate and invade (80). These differences may be due to changes in matrix stiffness or porosity that are transduced into the cells *via* integrin and focal adhesion signalling, consequently affecting processes, such as signalling responses and gene expression (80,95). This is underpinned by the effect of matrix pore size on cell migration. For example, small pores that permit migration can promote short-term cell invasion due to immediate cell surface contact and attachment (96–98). However, migration through small pores can depend upon the proteolytic capacity of the cells to remodel ECM (99). On the other hand, larger pores enhance long-term invasion due to their increased penetrability (97). It is challenging to modulate one specific ECM feature, without affecting other characteristics. Stiffness, pliability and porosity within 3D hydrogels often cannot be regulated independently (e.g. by modulating protein concentration, pH or polymerization temperature). The distinct roles of stiffness and porosity have been emphasized by embedding human glioma cells into polyacrylamide channels of varying stiffness and distinct widths allowing independent modulation of stiffness and porosity. In this study, the authors showed that small pore sizes of stiff material enhance invasion (96). Stiffened matrices



increased the contraction of the actomyosin cytoskeleton, while narrow channels physically constrained migrating cells, which in combination focussed directional cell movement (96). These experiments underline the role of distinct biomechanical stimuli in cell proliferation, survival and motility. Synthetic materials are easier to remodel and manipulate; however, their *in vivo* fidelity is limited. Hence, it is necessary to design experimental systems containing ECM proteins amenable to specific manipulation of single matrix features at the ultrastructural level.

As such, in the following section, we provide a basic guide on how to best choose a model, governed by the cancer aspect in question. It is important to note that results obtained from complex *in vitro*, but also *in vivo* models, may be difficult to interpret, and be prone to strong variation across samples or produce artefacts. Moreover, we must consider that 2D, 3D and *in vivo* models of disease only recapitulate distinct aspects of the disease in question, and that a combination of assays may be necessary to provide the overarching assessment of the biology under investigation.

### Selecting the appropriate system

In order to analyse commonly addressed mechanistic questions, such as those assessing changes in cell proliferation, survival or migration, 2D assessments provide early advantages, in which accessibility, facilitated molecular manipulation, such as transfections and clonal selection, and simplified imaging set-ups can be utilized (Figure 2A). It is important to note, however, that while 2D examinations can support robust and high-throughput readouts, some cancer behaviours may only be revealed when assessed in a 3D context. Therefore, the choice to move to 3D systems is one in which an increase in heterogeneity, complexity or dimension is required to permit the analysis of phenomena, such as cell polarity or tissue-like architecture. In order to maximize the output from 3D *in vitro* models of cancer biology, we provide a simplified decision tree (Figure 2A). To this end, we have split the 3D selection criteria into four basic themes, namely spheroids in ECM-free cultures, CDMs, hydrogels and microfluidics (Figures 1, Figure 2A and Table I). Thus, we assist in choosing the most appropriate system, depending on the biological question of interest, where *in vitro* assessment can be used to achieve rapid readouts that may guide the *in vivo* arm of research with reduced time or cost, but also accepting an incomplete approximation of the *in vivo* situation as current *in vitro* set-ups are not always able to simulate the high tissue complexity and cell–ECM spacing found *in vivo*.

Spheroid model systems offer the potential for relatively easy molecular or genetic intervention and provide readouts for basic tumour growth and survival data, as well as specific architectures within a 3D *in vitro* setting (Figure 2A, ECM-free spheroid culture). For example, primary mouse mammary spheroids or MCF10A spheroids replicate the epithelial architecture of breast morphogenesis (26,100), while duodenal crypt cultures allow assessment of homeostasis or genetic control of intestinal regeneration (101–104). Multicellular tumour spheroids simulate features of tumour nodule formation *in vivo*, such as hypoxic and acidic gradients towards the spheroid centre (105,106), thereby establishing several cell populations within the spheroid, analogous to tumour formation *in vivo*, i.e. outer proliferating cells and inner dormant cells that *in vivo* show resistance to conventional cytostatic therapy (107,108). Thus, multicellular tumour spheroids can be used to develop therapeutic approaches against both proliferating cells and dormant tumour cells (109). Furthermore, spheroids consisting of several cell types can provide readouts for cell–stroma interactions within tumours (110–113). For example, the co-culture of prostate cancer cells with osteoblasts and endothelial cells has been used to mimic the bone metastatic niche of prostate cancer (110).

CDMs provide an ideal, rapid and highly informative platform to examine reciprocal feedback between cells and stromal ECM (114). They are not only a de-cellularized matrix scaffold for cell–ECM adhesion, but also incorporate various signalling cues, such as growth factors and cytokines. Their composition can also be

manipulated through modification of the culture medium during formation (Figure 2A, CDMs). For example, ascorbic acid can be used to enhance the collagen content (115), while fibrillar fibronectin produced by fibroblasts can also be increased in this context (116). In this way, the role and regulation of  $\alpha 5 \beta 1$  integrin, which functions as a key fibronectin receptor, has been investigated in the context of breast (30,117), ovarian (31,32,117,118) and fibrosarcoma (30) cell motility.

Although models of thinner ECM, such as those provided by CDMs, offer many advantages, including ease of imaging (93), they do not allow cell integration into the scaffold or assessment of deep cell invasion, which requires a thicker matrix (Figure 2A, hydrogels). Hydrogels, such as Matrigel or collagen I matrices, can be used to examine invasion dynamics in a 3D environment and provide readouts on cancer cell type-specific behaviour, such as migration, invasion and cell–ECM interactions (119,120). 3D matrix embedding of cancer cells within or on top of matrices can be used to monitor invasion depth and modes of invasion, such as single or collective invasion (73,121,122). More complex hydrogels involving matrix spiked with further components, such as fibronectin, can be used to create a more diverse microenvironment (118,123), while co-cultural cross-talk of different cell types within hydrogels, such as fibroblasts (124–126), macrophages (127) or stellate cells (128,129), can be used to examine interdependent aspects of tumour behaviour in 3D.

Lastly, cellular behaviour in response to shear stress and liquid flow resistance can best be studied in microfluidic devices, which, due to their dynamic perfusion, are able to simulate forces generated by blood flow (Figure 2A, microfluidics). For example, cancer cell motility and chemotaxis can be quantified by seeding cells into chambers that are exposed to chemotactic gradients, which can be coupled to live imaging of cell migration through the microchannels (130). Furthermore, precise control over the perfusion dynamics in microfluidics permits the recapitulation of clinically relevant drug dosages to determine parameters for optimal dosage concentrations, combinations and sequences (131,132).

It is important to note that no one system outlined in this brief, non-exhaustive decision tree can provide all the required insights needed to understand complex biological questions. Therefore, combination of multiple *in vitro* and *in vivo* systems, which inform each other (Figure 2A, grey-dashed arrows), may be necessary to provide a comprehensive perspective in any given scenario.

### Physical combination of 3D *in vitro* systems can improve assay fidelity

In line with this concept, we have created a network map (see Figure 2B), in which we propose, apart from using two 3D *in vitro* systems in parallel, the physical combination of the strengths of distinct 3D systems to overcome their respective weaknesses. Here, we highlight the potential advantages of each system with associated examples of their disadvantages. Where we envisage a limitation, we suggest the system we believe is best suited to allay this caveat, if used in combination, providing examples where this has been successfully applied.

To address the reduced scaffolding, ECM diversity and biomechanical stimulation of spheroids for instance, physical combination of spheroids with CDMs or hydrogels (Figure 2B, orange and blue arrows from ECM-free spheroid culture to CDMs and hydrogels, respectively) can mimic 3D architecture of primary tumours within an ECM network (133,134). Similarly, spheroids have been embedded into 3D organotypic matrices (Figure 2B, blue arrow from ECM-free spheroid culture to hydrogels) to confer co-cultural cross-talk with other cell types in a 3D environment (128,135–137). An artificial skin model has been developed in which keratinocytes seeded on top of a collagen-fibroblast matrix form epidermal layers above a dermal-like compartment of collagen and fibroblasts ultimately mimicking the human skin, to demonstrate niche-specific success rates of drug combination therapy (138). Moreover, direct spheroid formation from single cells has been accomplished within microfluidic devices under dynamic perfusion and shear stress (Figure 2B, green arrows from ECM-free

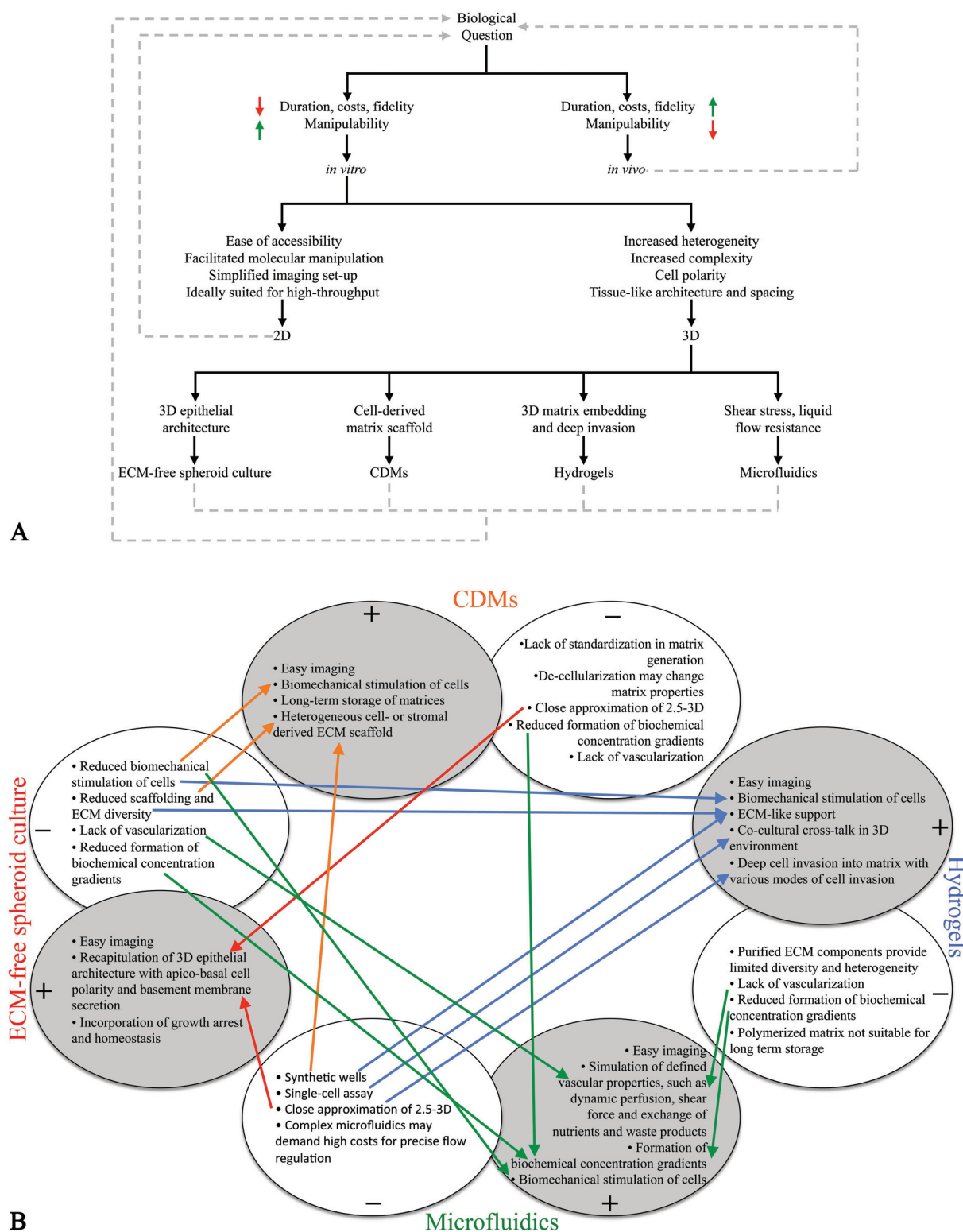


**Fig. 2.** A decision tree (**A**) and a network map (**B**) to aid in the choice of appropriate *in vitro* or *in vivo* model systems. (**A**) Based on a given biological question within the decision tree the first choice between *in vitro* and *in vivo* model systems may be influenced by factors, such as costs, duration, the capacity for manipulation or the required level of fidelity. A second decision is made between 2D and 3D *in vitro* systems, whereby 2D systems provide several advantages, including ease of accessibility, uniformity across the sample, simplified imaging set-ups and suitability for high-throughput screening. Lastly, the increased heterogeneity, depth and complexity of 3D systems present an additional choice from the four themes discussed, depending on the biological question of interest, i.e. 3D epithelial architecture in ECM-free spheroid culture (3D spheroids generated and propagated in the absence of an ECM-derived support matrix), de-cellularized scaffolds in CDMs, 3D matrix embedding on or within hydrogels or shear stress and dynamic perfusion in microfluidics. Finally, upon analysis the experimental results feed back to the original biological question of interest. (**B**) Network map depicting selected advantages (+) and disadvantages (-) of 3D *in vitro* systems and suggested combinations, which can compensate the weaknesses of one system by the strengths of another. ECM-free spheroid culture (3D spheroids generated and propagated in the absence of an ECM-derived support matrix, red), CDMs (orange), hydrogels (blue) and microfluidics (green). Colour-coded arrows pair assays as a guide for higher fidelity experimental design. The colour coding of the arrows was chosen to support clarity without any additional meaning.

spheroid culture to microfluidics), by trapping the cells in moulds attached to the microchannels. This system can then be instantly used as a drug-screening platform with dynamic perfusion (110,139).

In order to remove artificial surfaces within microfluidics, the channels can be coated with protein substrates, such as ECM components to facilitate cell attachment and migration (140,141) (Figure 2B, blue arrows from microfluidics to hydrogels). These matrix substrates can also be used for endothelial cell adhesion and it has been shown that macrophages stimulate cancer cell migration through the matrix substrate and the endothelial layer simulating tumour cell intravasation into blood vessels *in vivo* (142).

The combination of spheroids embedded into a hydrogel within a microfluidic device shows great potential for 3D high-throughput screens. Microfluidics can simulate vascular properties, such as dynamic perfusion, shear stress and exchange of nutrients and waste products, whereas spheroids recapitulate 3D cellular architecture and hydrogels mediate 3D scaffolding (143). Within this system, breast cancer cells were grown in Matrigel to form multicellular tumour spheroids, then transferred to a microfluidic system to simulate mechanical stress and constant exchange of nutrients, cell-secreted substances and drugs. As imaging is possible over the whole course of the experiment, such systems can be used in a high-throughput manner to recapitulate tumour progression or its inhibition within a dynamic environment (143).

As the complexity of 3D *in vitro* systems increases, we approach a situation where fidelity is high, whereas cost and duration can remain relatively low (Figure 2A). Such systems are ideally suited to test in 3D the effects of new drugs on basic cellular readouts, such as viability or migration and invasion, or screen a library of patient-derived samples for effective drug concentrations and combinations.

## Future directions

To our knowledge, a direct and physical combination of the strengths of CDMs (Figure 2B, CDMs as heterogeneous cell-derived ECM scaffold) and hydrogels (Figure 2B, hydrogels as thick matrix for deep cell invasion and co-cultural cross-talk) has not yet been performed. Rather, both systems are used in parallel to address cell–ECM adhesions and 2.5D migration across CDMs, compared with 3D invasion and co-cultural cross-talk in hydrogels (2,118,125,144). An emerging topic originating from tissue engineering is the use of de-cellularized tissue-derived matrices (TDMs) (145). De-cellularization with detergents removes the cells, while leaving an almost native ECM scaffold behind. Recently, lung cells seeded onto a de-cellularized lung TDM were shown to form perfusable tumour nodules reminiscent in structure to primary human lung tumours (77). Alternatively, cancer cell invasion into whole tissues can be performed without any de-cellularization, using an intact stroma. In addition to the use of leiomyoma tissue (75,76), carcinoma cells have been embedded into Matrigel adjacent to mouse brain slices to image cancer cell invasion in the brain. In this way, the interactions of cancer cells with host cells, such as glia, have been described, which, importantly, is difficult to accomplish in an intravital setting due to limitations caused by the skull (146).

We envisage that complex substrates such as TDMs or whole tissues will be used more frequently in the future when addressing cancer cell behaviour and treatment *in vitro*. These substrates provide a high fidelity in mimicking native cancer cell–stroma interaction. Furthermore, cancer cells and TDMs can be combined in clinically relevant ways to study invasion and colonization at secondary sites, for example, metastasis of breast cancer cells into lung TDM or invasion of pancreatic or colon cancer cells into liver sections or liver TDM. However, a clear downside of TDMs and whole tissues is that not all these substrates can be readily harvested from human patients, and thus require extensive use of animal tissue with a concomitant step backwards in fidelity. In addition, the current lack of standardization in TDM generation reduces assay reproducibility and thus limits the widespread use of TDMs in the pharmaceutical industry. Nevertheless, due to their high level of fidelity, TDMs and whole tissues may be promising tools in personalized therapeutic approaches (79,147).

Lastly, while several 2D and 3D *in vitro* models have been employed to simulate blood vessel formation or defined vascular properties (148,149), a clear recapitulation of a complex, perfusable circulatory system, which would be required to study phenomena such as drug delivery or clearance *in vitro*, is still lacking. Recent advances in microfluidic systems include the formation of stable, lumenized structures from endothelial cells growing into a fibrin- or collagen-filled microfluidic device (150–154). These structures have been shown to be perfusable by microfluidic flow and resistant to shear stress and have been used to recapitulate several aspects of perfused blood vessel networks *in vivo*, such as coverage by pericytes (154), or leukocyte adhesion to the endothelium (154) and thrombus formation (150) upon inflammatory stimulation. The embedding of such stable and perfusable vessel systems within a malleable *in vitro* tumour microenvironment composed of cancer cells, stromal cells and ECM should improve our understanding of processes leading to tissue malperfusion to better guide drug delivery *in vivo*.

Thus, we suggest the following directions into which 3D *in vitro* systems may move in the future. On the one hand, physical combinations of 3D *in vitro* systems offer the possibility to test early phase drugs in a high-throughput setting or screen a large patient cohort, while on the other hand, highly specific assays, such as use of TDMs, offer guides within personalized medicine for individual cases. Furthermore, the development of sophisticated *in vitro* tumour microenvironments may help to reveal mechanisms of drug delivery, and its obstruction in tumours *in vivo*. In conclusion, it is important to take into consideration that 2D, 3D and *in vivo* systems may only model distinct pathological aspects of the disease in question, and that a combination of several assays may be necessary to provide the overarching assessment of the biology under investigation.

## Funding

Australian Research Council (ARC 9); Cancer Institute of New South Wales (CINSW 49); Cancer Council New South Wales (14-08); National Health and Medical Research Council (NHMRC 147).

## Acknowledgements

The authors would like to thank Dr E.van Dam, Dr K.Moran-Jones, Dr A.Cazet, K.Halfter and Dr B.Browne for critical reading of the manuscript.

*Conflict of Interest Statement:* None declared.

## References

1. Timpson, P. *et al.* (2011) Spatial regulation of RhoA activity during pancreatic cancer cell invasion driven by mutant p53. *Cancer Res.*, **71**, 747–757.
2. McGhee, E.J. *et al.* (2011) FLIM-FRET imaging *in vivo* reveals 3D-environment spatially regulates RhoGTPase activity during cancer cell invasion. *Small GTPases*, **2**, 239–244.
3. Artym, V.V. *et al.* (2006) Dynamic interactions of cortactin and membrane type 1 matrix metalloproteinase at invadopodia: defining the stages of invadopodia formation and function. *Cancer Res.*, **66**, 3034–3043.
4. Tolde, O. *et al.* (2010) The structure of invadopodia in a complex 3D environment. *Eur. J. Cell Biol.*, **89**, 674–680.
5. Schachner, H. *et al.* (2012) Tissue inducible Lifeact expression allows visualization of actin dynamics *in vivo* and ex vivo. *Eur. J. Cell Biol.*, **91**, 923–929.
6. Gligorijevic, B. *et al.* (2012) N-WASP-mediated invadopodium formation is involved in intravasation and lung metastasis of mammary tumors. *J. Cell Sci.*, **125**(Pt 3), 724–734.
7. Destaing, O. *et al.* (2003) Podosomes display actin turnover and dynamic self-organization in osteoclasts expressing actin-green fluorescent protein. *Mol. Biol. Cell*, **14**, 407–416.
8. Van Goethem, E. *et al.* (2011) Macrophage podosomes go 3D. *Eur. J. Cell Biol.*, **90**, 224–236.
9. Linder, S. *et al.* (2003) Podosomes: adhesion hot-spots of invasive cells. *Trends Cell Biol.*, **13**, 376–385.
10. Fraley, S.I. *et al.* (2010) A distinctive role for focal adhesion proteins in three-dimensional cell motility. *Nat. Cell Biol.*, **12**, 598–604.



11. Kubow, K.E. *et al.* (2011) Reducing background fluorescence reveals adhesions in 3D matrices. *Nat. Cell Biol.*, **13**, 3–5; author reply 5.
12. Tolde, O. *et al.* (2012) Dynamics and morphology of focal adhesions in complex 3D environment. *Folia Biol. (Praha)*, **58**, 177–184.
13. Cukierman, E. *et al.* (2001) Taking cell-matrix adhesions to the third dimension. *Science*, **294**, 1708–1712.
14. Hakkinen, K.M. *et al.* (2011) Direct comparisons of the morphology, migration, cell adhesions, and actin cytoskeleton of fibroblasts in four different three-dimensional extracellular matrices. *Tissue Eng. Part A*, **17**, 713–724.
15. Geraldo, S. *et al.* (2012) Do cancer cells have distinct adhesions in 3D collagen matrices and *in vivo*? *Eur. J. Cell Biol.*, **91**, 930–937.
16. Weigelin, B. *et al.* (2012) Intravital third harmonic generation microscopy of collective melanoma cell invasion: principles of interface guidance and microvesicle dynamics. *Intravital*, **1**, 32–43.
17. Doyle, A.D. *et al.* (2009) One-dimensional topography underlies three-dimensional fibrillar cell migration. *J. Cell Biol.*, **184**, 481–490.
18. Petrie, R.J. *et al.* (2009) Random versus directionally persistent cell migration. *Nat. Rev. Mol. Cell Biol.*, **10**, 538–549.
19. Debnath, J. *et al.* (2003) Morphogenesis and oncogenesis of MCF-10A mammary epithelial acini grown in three-dimensional basement membrane cultures. *Methods*, **30**, 256–268.
20. Debnath, J. *et al.* (2003) Akt activation disrupts mammary acinar architecture and enhances proliferation in an mTOR-dependent manner. *J. Cell Biol.*, **163**, 315–326.
21. Herr, R. *et al.* (2011) A novel MCF-10A line allowing conditional oncogene expression in 3D culture. *Cell Commun. Signal.*, **9**, 17.
22. Woods Ignatoski, K.M. *et al.* (2005) Cooperative interactions of HER-2 and HPV-16 oncoproteins in the malignant transformation of human mammary epithelial cells. *Neoplasia*, **7**, 788–798.
23. Brummer, T. *et al.* (2006) Increased proliferation and altered growth factor dependence of human mammary epithelial cells overexpressing the Gab2 docking protein. *J. Biol. Chem.*, **281**, 626–637.
24. Bennett, H.L. *et al.* (2008) Gab2 and Src co-operate in human mammary epithelial cells to promote growth factor independence and disruption of acinar morphogenesis. *Oncogene*, **27**, 2693–2704.
25. Bentires-Alj, M. *et al.* (2006) A role for the scaffolding adapter GAB2 in breast cancer. *Nat. Med.*, **12**, 114–121.
26. Caldon, C.E. *et al.* (2008) The helix-loop-helix protein Id1 requires cyclin D1 to promote the proliferation of mammary epithelial cell acini. *Cancer Res.*, **68**, 3026–3036.
27. Zhan, L. *et al.* (2008) Deregulation of scribble promotes mammary tumorigenesis and reveals a role for cell polarity in carcinoma. *Cell*, **135**, 865–878.
28. Zhang, Y. *et al.* (2011) Mutant p53 disrupts MCF-10A cell polarity in three-dimensional culture via epithelial-to-mesenchymal transitions. *J. Biol. Chem.*, **286**, 16218–16228.
29. Deakin, N.O. *et al.* (2012) Paxillin and Hic-5 interaction with vinculin is differentially regulated by Rac1 and RhoA. *PLoS One*, **7**, e37990.
30. Jacquemet, G. *et al.* (2013) RCP-driven  $\alpha 5 \beta 1$  recycling suppresses Rac and promotes RhoA activity via the RacGAP1-IQGAP1 complex. *J. Cell Biol.*, **202**, 917–935.
31. Caswell, P.T. *et al.* (2008) Rab-coupling protein coordinates recycling of  $\alpha 5 \beta 1$  integrin and EGFR1 to promote cell migration in 3D microenvironments. *J. Cell Biol.*, **183**, 143–155.
32. Caswell, P.T. *et al.* (2007) Rab25 associates with  $\alpha 5 \beta 1$  integrin to promote invasive migration in 3D microenvironments. *Dev. Cell*, **13**, 496–510.
33. Pickl, M. *et al.* (2009) Comparison of 3D and 2D tumor models reveals enhanced HER2 activation in 3D associated with an increased response to trastuzumab. *Oncogene*, **28**, 461–468.
34. Serebriiskii, I. *et al.* (2008) Fibroblast-derived 3D matrix differentially regulates the growth and drug-responsiveness of human cancer cells. *Matrix Biol.*, **27**, 573–585.
35. Talukdar, S. *et al.* (2012) A non-mulberry silk fibroin protein based 3D in vitro tumor model for evaluation of anticancer drug activity. *Adv. Funct. Mater.*, **22**, 4778–4788.
36. Longati, P. *et al.* (2013) 3D pancreatic carcinoma spheroids induce a matrix-rich, chemoresistant phenotype offering a better model for drug testing. *BMC Cancer*, **13**, 95.
37. Loessner, D. *et al.* (2010) Bioengineered 3D platform to explore cell-ECM interactions and drug resistance of epithelial ovarian cancer cells. *Biomaterials*, **31**, 8494–8506.
38. Howe, G.A. *et al.* (2012)  $\beta 1$  integrin: an emerging player in the modulation of tumorigenesis and response to therapy. *Cell Adh. Migr.*, **6**, 71–77.
39. Sethi, T. *et al.* (1999) Extracellular matrix proteins protect small cell lung cancer cells against apoptosis: a mechanism for small cell lung cancer growth and drug resistance *in vivo*. *Nat. Med.*, **5**, 662–668.
40. Hsieh, Y.T. *et al.* (2013) Integrin  $\alpha 4$  blockade sensitizes drug resistant pre-B acute lymphoblastic leukemia to chemotherapy. *Blood*, **121**, 1814–1818.
41. Janouskova, H. *et al.* (2012) Integrin  $\alpha 5 \beta 1$  plays a critical role in resistance to temozolomide by interfering with the p53 pathway in high-grade glioma. *Cancer Res.*, **72**, 3463–3470.
42. Borovski, T. *et al.* (2011) Cancer stem cell niche: the place to be. *Cancer Res.*, **71**, 634–639.
43. Lu, P. *et al.* (2012) The extracellular matrix: a dynamic niche in cancer progression. *J. Cell Biol.*, **196**, 395–406.
44. Friedl, P. *et al.* (2011) Cancer invasion and the microenvironment: plasticity and reciprocity. *Cell*, **147**, 992–1009.
45. Edward, M. *et al.* (2005) Tumour regulation of fibroblast hyaluronan expression: a mechanism to facilitate tumour growth and invasion. *Carcinogenesis*, **26**, 1215–1223.
46. Imamura, T. *et al.* (1995) Quantitative analysis of collagen and collagen subtypes I, III, and V in human pancreatic cancer, tumor-associated chronic pancreatitis, and alcoholic chronic pancreatitis. *Pancreas*, **11**, 357–364.
47. Devy, J. *et al.* (2010) Elastin-derived peptides enhance melanoma growth *in vivo* by upregulating the activation of Mcol-A (MMP-1) collagenase. *Br. J. Cancer*, **103**, 1562–1570.
48. Sanchez, C.G. *et al.* (2011) Activation of autophagy in mesenchymal stem cells provides tumor stromal support. *Carcinogenesis*, **32**, 964–972.
49. Bissell, M.J. *et al.* (2011) Why don't we get more cancer? A proposed role of the microenvironment in restraining cancer progression. *Nat. Med.*, **17**, 320–329.
50. Chang, P.H. *et al.* (2012) Activation of Robo1 signaling of breast cancer cells by Slit2 from stromal fibroblast restrains tumorigenesis via blocking PI3K/Akt/ $\beta$ -catenin pathway. *Cancer Res.*, **72**, 4652–4661.
51. Straussman, R. *et al.* (2012) Tumour micro-environment elicits innate resistance to RAF inhibitors through HGF secretion. *Nature*, **487**, 500–504.
52. Brown, E. *et al.* (2003) Dynamic imaging of collagen and its modulation in tumors *in vivo* using second-harmonic generation. *Nat. Med.*, **9**, 796–800.
53. Spivak-Kroizman, T.R. *et al.* (2013) Hypoxia triggers hedgehog-mediated tumor-stromal interactions in pancreatic cancer. *Cancer Res.*, **73**, 3235–3247.
54. Nobis, M. *et al.* (2013) Intravital FLIM-FRET imaging reveals dasatinib-induced spatial control of src in pancreatic cancer. *Cancer Res.*, **73**, 4674–4686.
55. Jacobetz, M.A. *et al.* (2013) Hyaluronan impairs vascular function and drug delivery in a mouse model of pancreatic cancer. *Gut*, **62**, 112–120.
56. Provenzano, P.P. *et al.* (2012) Enzymatic targeting of the stroma ablates physical barriers to treatment of pancreatic ductal adenocarcinoma. *Cancer Cell*, **21**, 418–429.
57. Ramanujan, S. *et al.* (2002) Diffusion and convection in collagen gels: implications for transport in the tumor interstitium. *Biophys. J.*, **83**, 1650–1660.
58. Kihara, T. *et al.* (2013) Measurement of biomolecular diffusion in extracellular matrix condensed by fibroblasts using fluorescence correlation spectroscopy. *PLoS One*, **8**, e82382.
59. Pluen, A. *et al.* (2001) Role of tumor-host interactions in interstitial diffusion of macromolecules: cranial vs. subcutaneous tumors. *Proc. Natl Acad. Sci. USA*, **98**, 4628–4633.
60. Netti, P.A. *et al.* (2000) Role of extracellular matrix assembly in interstitial transport in solid tumors. *Cancer Res.*, **60**, 2497–2503.
61. Olive, K.P. *et al.* (2009) Inhibition of Hedgehog signaling enhances delivery of chemotherapy in a mouse model of pancreatic cancer. *Science*, **324**, 1457–1461.
62. Stylianopoulos, T. *et al.* (2012) Causes, consequences, and remedies for growth-induced solid stress in murine and human tumors. *Proc. Natl Acad. Sci. USA*, **109**, 15101–15108.
63. Barsky, S.H. *et al.* (1982) Increased content of Type V Collagen in desmoplasia of human breast carcinoma. *Am. J. Pathol.*, **108**, 276–283.
64. Clavel, C. *et al.* (1989) Detection by *in situ* hybridization of messenger RNAs of collagen types I and IV in murine mammary cancer. *Int. J. Cancer*, **44**, 548–553.
65. Li, H.X. *et al.* (2013) Expression of  $\alpha \beta 6$  integrin and collagen fibre in oral squamous cell carcinoma: association with clinical outcomes and prognostic implications. *J. Oral Pathol. Med.*, **42**, 547–556.
66. Samuel, M.S. *et al.* (2011) Actomyosin-mediated cellular tension drives increased tissue stiffness and  $\beta$ -catenin activation to induce epidermal hyperplasia and tumor growth. *Cancer Cell*, **19**, 776–791.
67. Ibbetson, S.J. *et al.* (2013) Mechanotransduction pathways promoting tumor progression are activated in invasive human squamous cell carcinoma. *Am. J. Pathol.*, **183**, 930–937.

68. Provenzano, P.P. *et al.* (2008) Collagen density promotes mammary tumor initiation and progression. *BMC Med.*, **6**, 11.
69. Levental, K.R. *et al.* (2009) Matrix crosslinking forces tumor progression by enhancing integrin signaling. *Cell*, **139**, 891–906.
70. Provenzano, P.P. *et al.* (2006) Collagen reorganization at the tumor-stromal interface facilitates local invasion. *BMC Med.*, **4**, 38.
71. Cox, T.R. *et al.* (2013) LOX-mediated collagen crosslinking is responsible for fibrosis-enhanced metastasis. *Cancer Res.*, **73**, 1721–1732.
72. Nyström, M.L. *et al.* (2005) Development of a quantitative method to analyse tumour cell invasion in organotypic culture. *J. Pathol.*, **205**, 468–475.
73. Muller, P.A. *et al.* (2009) Mutant p53 drives invasion by promoting integrin recycling. *Cell*, **139**, 1327–1341.
74. Suri, S. *et al.* (2010) Cell-laden hydrogel constructs of hyaluronic acid, collagen, and laminin for neural tissue engineering. *Tissue Eng. Part A*, **16**, 1703–1716.
75. Nurmenniemi, S. *et al.* (2009) A novel organotypic model mimics the tumor microenvironment. *Am. J. Pathol.*, **175**, 1281–1291.
76. Teppo, S. *et al.* (2013) The hypoxic tumor microenvironment regulates invasion of aggressive oral carcinoma cells. *Exp. Cell Res.*, **319**, 376–389.
77. Mishra, D.K. *et al.* (2012) Human lung cancer cells grown on acellular rat lung matrix create perfusable tumor nodules. *Ann. Thorac. Surg.*, **93**, 1075–1081.
78. Siolas, D. *et al.* (2013) Patient-derived tumor xenografts: transforming clinical samples into mouse models. *Cancer Res.*, **73**, 5315–5319.
79. Tentler, J.J. *et al.* (2012) Patient-derived tumour xenografts as models for oncology drug development. *Nat. Rev. Clin. Oncol.*, **9**, 338–350.
80. Schedin, P. *et al.* (2011) Mammary gland ECM remodeling, stiffness, and mechanosignaling in normal development and tumor progression. *Cold Spring Harb. Perspect. Biol.*, **3**, a003228.
81. Discher, D.E. *et al.* (2005) Tissue cells feel and respond to the stiffness of their substrate. *Science*, **310**, 1139–1143.
82. Lam, W.A. *et al.* (2010) Extracellular matrix rigidity modulates neuroblastoma cell differentiation and N-myc expression. *Mol. Cancer*, **9**, 35.
83. Wells, R.G. (2008) The role of matrix stiffness in regulating cell behavior. *Hepatology*, **47**, 1394–1400.
84. Ulrich, T.A. *et al.* (2009) The mechanical rigidity of the extracellular matrix regulates the structure, motility, and proliferation of glioma cells. *Cancer Res.*, **69**, 4167–4174.
85. Boghaert, E. *et al.* (2012) Host epithelial geometry regulates breast cancer cell invasiveness. *Proc. Natl Acad. Sci. USA*, **109**, 19632–19637.
86. Radisky, D.C. *et al.* (2013) Regulation of mechanical stress by mammary epithelial tissue structure controls breast cancer cell invasion. *Oncotarget*, **4**, 498–499.
87. Menon, S. *et al.* (2011) Cancer cell invasion is enhanced by applied mechanical stimulation. *PLoS One*, **6**, e17277.
88. Baker, A.M. *et al.* (2013) Lysyl oxidase enzymatic function increases stiffness to drive colorectal cancer progression through FAK. *Oncogene*, **32**, 1863–1868.
89. Baker, A.M. *et al.* (2013) Lysyl oxidase plays a critical role in endothelial cell stimulation to drive tumor angiogenesis. *Cancer Res.*, **73**, 583–594.
90. Schrader, J. *et al.* (2011) Matrix stiffness modulates proliferation, chemotherapeutic response, and dormancy in hepatocellular carcinoma cells. *Hepatology*, **53**, 1192–1205.
91. Zusiak, S. *et al.* (2013) Multiwell stiffness assay for the study of cell responsiveness to cytotoxic drugs. *Biotechnol. Bioeng.*, **111**, 396–403.
92. Soofi, S.S. *et al.* (2009) The elastic modulus of Matrigel as determined by atomic force microscopy. *J. Struct. Biol.*, **167**, 216–219.
93. Soucy, P.A. *et al.* (2011) Microelastic properties of lung cell-derived extracellular matrix. *Acta Biomater.*, **7**, 96–105.
94. Grinnell, F. *et al.* (2010) Cell motility and mechanics in three-dimensional collagen matrices. *Annu. Rev. Cell Dev. Biol.*, **26**, 335–361.
95. Provenzano, P.P. *et al.* (2009) Matrix density-induced mechanoregulation of breast cell phenotype, signaling and gene expression through a FAK-ERK linkage. *Oncogene*, **28**, 4326–4343.
96. Pathak, A. *et al.* (2012) Independent regulation of tumor cell migration by matrix stiffness and confinement. *Proc. Natl Acad. Sci. USA*, **109**, 10334–10339.
97. Murphy, C.M. *et al.* (2010) Understanding the effect of mean pore size on cell activity in collagen-glycosaminoglycan scaffolds. *Cell Adh. Migr.*, **4**, 377–381.
98. Harley, B.A. *et al.* (2008) Microarchitecture of three-dimensional scaffolds influences cell migration behavior via junction interactions. *Biophys. J.*, **95**, 4013–4024.
99. Wolf, K. *et al.* (2013) Physical limits of cell migration: control by ECM space and nuclear deformation and tuning by proteolysis and traction force. *J. Cell Biol.*, **201**, 1069–1084.
100. Jechlinger, M. *et al.* (2009) Regulation of transgenes in three-dimensional cultures of primary mouse mammary cells demonstrates oncogene dependence and identifies cells that survive deinduction. *Genes Dev.*, **23**, 1677–1688.
101. Sato, T. *et al.* (2009) Single Lgr5 stem cells build crypt-villus structures *in vitro* without a mesenchymal niche. *Nature*, **459**, 262–265.
102. Sato, T. *et al.* (2011) Long-term expansion of epithelial organoids from human colon, adenoma, adenocarcinoma, and Barrett's epithelium. *Gastroenterology*, **141**, 1762–1772.
103. Myant, K.B. *et al.* (2013) ROS production and NF- $\kappa$ B activation triggered by RAC1 facilitate WNT-driven intestinal stem cell proliferation and colorectal cancer initiation. *Cell Stem Cell*, **12**, 761–773.
104. Johnsson, A.K. *et al.* (2014) The Rac-FRET mouse reveals tight spatiotemporal control of Rac activity in primary cells and tissues. *Cell Rep.*, **6**, 1153–1164.
105. Carlsson, J. *et al.* (1988) Relations between pH, oxygen partial pressure and growth in cultured cell spheroids. *Int. J. Cancer*, **42**, 715–720.
106. Friedrich, J. *et al.* (2009) Spheroid-based drug screen: considerations and practical approach. *Nat. Protoc.*, **4**, 309–324.
107. Kreso, A. *et al.* (2013) Variable clonal repopulation dynamics influence chemotherapy response in colorectal cancer. *Science*, **339**, 543–548.
108. Patel, S.A. *et al.* (2012) Delineation of breast cancer cell hierarchy identifies the subset responsible for dormancy. *Sci. Rep.*, **2**, 906.
109. Wenzel, C. *et al.* (2014) 3D high-content screening for the identification of compounds that target cells in dormant tumor spheroid regions. *Exp. Cell Res.*, **323**, 131–143.
110. Hsiao, A.Y. *et al.* (2009) Microfluidic system for formation of PC-3 prostate cancer co-culture spheroids. *Biomaterials*, **30**, 3020–3027.
111. Ingram, M. *et al.* (2010) Tissue engineered tumor models. *Biotech. Histochem.*, **85**, 213–229.
112. Bratt-Leal, A.M. *et al.* (2011) Magnetic manipulation and spatial patterning of multi-cellular stem cell aggregates. *Integr. Biol. (Camb.)*, **3**, 1224–1232.
113. Mattix, B.M. *et al.* (2014) Janus magnetic cellular spheroids for vascular tissue engineering. *Biomaterials*, **35**, 949–960.
114. Green, J.A. *et al.* (2007) Three-dimensional microenvironments modulate fibroblast signaling responses. *Adv. Drug Deliv. Rev.*, **59**, 1293–1298.
115. Grinnell, F. *et al.* (1989) Collagen processing, crosslinking, and fibril bundle assembly in matrix produced by fibroblasts in long-term cultures supplemented with ascorbic acid. *Exp. Cell Res.*, **181**, 483–491.
116. Dzamba, B.J. *et al.* (1991) Arrangement of cellular fibronectin in non-collagenous fibrils in human fibroblast cultures. *J. Cell Sci.*, **100**(Pt 3), 605–612.
117. Zech, T. *et al.* (2011) The Arp2/3 activator WASH regulates  $\alpha 5 \beta 1$ -integrin-mediated invasive migration. *J. Cell Sci.*, **124**(Pt 22), 3753–3759.
118. Dozynkiewicz, M.A. *et al.* (2012) Rab25 and CLIC3 collaborate to promote integrin recycling from late endosomes/lysosomes and drive cancer progression. *Dev. Cell*, **22**, 131–145.
119. Sodek, K.L. *et al.* (2008) Collagen I but not Matrigel matrices provide an MMP-dependent barrier to ovarian cancer cell penetration. *BMC Cancer*, **8**, 223.
120. Hsieh, A.C. *et al.* (2012) The translational landscape of mTOR signalling steers cancer initiation and metastasis. *Nature*, **485**, 55–61.
121. Tang, H. *et al.* (2013) Loss of Scar/WAVE complex promotes N-WASP- and FAK-dependent invasion. *Curr. Biol.*, **23**, 107–117.
122. Hennigan, R.F. *et al.* (1994) Fos-transformation activates genes associated with invasion. *Oncogene*, **9**, 3591–3600.
123. Calvo, F. *et al.* (2013) Mechanotransduction and YAP-dependent matrix remodelling is required for the generation and maintenance of cancer-associated fibroblasts. *Nat. Cell Biol.*, **15**, 637–646.
124. Timpson, P. *et al.* (2011) Organotypic collagen I assay: a malleable platform to assess cell behaviour in a 3-dimensional context. *J. Vis. Exp.*, **56**, e3089.
125. Timpson, P. *et al.* (2011) Imaging molecular dynamics *in vivo*—from cell biology to animal models. *J. Cell Sci.*, **124**(Pt 17), 2877–2890.
126. Gaggioli, C. *et al.* (2007) Fibroblast-led collective invasion of carcinoma cells with differing roles for RhoGTPases in leading and following cells. *Nat. Cell Biol.*, **9**, 1392–1400.
127. Linde, N. *et al.* (2012) Integrating macrophages into organotypic co-cultures: a 3D *in vitro* model to study tumor-associated macrophages. *PLoS One*, **7**, e40058.
128. Froeling, F.E. *et al.* (2009) Organotypic culture model of pancreatic cancer demonstrates that stromal cells modulate E-cadherin, beta-catenin, and Ezrin expression in tumor cells. *Am. J. Pathol.*, **175**, 636–648.
129. Kadaba, R. *et al.* (2013) Imbalance of desmoplastic stromal cell numbers drives aggressive cancer processes. *J. Pathol.*, **230**, 107–117.



130. Rao, S.M.N. *et al.* (2010) Demonstration of cancer cell migration using a novel microfluidic device. *J. Nanotech. Engineer. Med.*, **1**.
131. Kim, J. *et al.* (2012) A programmable microfluidic cell array for combinatorial drug screening. *Lab Chip*, **12**, 1813–1822.
132. Jastrzebska, E. *et al.* (2013) A microfluidic system to study the cytotoxic effect of drugs: the combined effect of celecoxib and 5-fluorouracil on normal and cancer cells. *Mikrochim. Acta*, **180**, 895–901.
133. Tamaki, M. *et al.* (1997) Implantation of C6 astrocytoma spheroid into collagen type I gels: invasive, proliferative, and enzymatic characterizations. *J. Neurosurg.*, **87**, 602–609.
134. Ho, W.J. *et al.* (2010) Incorporation of multicellular spheroids into 3-D polymeric scaffolds provides an improved tumor model for screening anticancer drugs. *Cancer Sci.*, **101**, 2637–2643.
135. Dolznig, H. *et al.* (2011) Modeling colon adenocarcinomas *in vitro* a 3D co-culture system induces cancer-relevant pathways upon tumor cell and stromal fibroblast interaction. *Am. J. Pathol.*, **179**, 487–501.
136. Lucas, K.M. *et al.* (2012) Modulation of NOXA and MCL-1 as a strategy for sensitizing melanoma cells to the BH3-mimetic ABT-737. *Clin. Cancer Res.*, **18**, 783–795.
137. Smalley, K.S. *et al.* (2008) *In vitro* three-dimensional tumor microenvironment models for anticancer drug discovery. *Expert Opin. Drug Discov.*, **3**, 1–10.
138. Vörsmann, H. *et al.* (2013) Development of a human three-dimensional organotypic skin-melanoma spheroid model for *in vitro* drug testing. *Cell Death Dis.*, **4**, e719.
139. Wu, L.Y. *et al.* (2008) Microfluidic self-assembly of tumor spheroids for anticancer drug discovery. *Biomed. Microdevices*, **10**, 197–202.
140. Chaw, K.C. *et al.* (2006) Three-dimensional (3D) extra-cellular matrix coating of a microfluidic device. *Internat. Memos Conference*, **34**, 747–751.
141. Annabi, N. *et al.* (2013) Hydrogel-coated microfluidic channels for cardiomyocyte culture. *Lab Chip*, **13**, 3569–3577.
142. Zervantonakis, I.K. *et al.* (2012) Three-dimensional microfluidic model for tumor cell intravasation and endothelial barrier function. *Proc. Natl Acad. Sci. USA*, **109**, 13515–13520.
143. Shin, C.S. *et al.* (2013) Development of an *in vitro* 3D tumor model to study therapeutic efficiency of an anticancer drug. *Mol. Pharm.*, **10**, 2167–2175.
144. Costa, P. *et al.* (2013) Integrin-specific control of focal adhesion kinase and RhoA regulates membrane protrusion and invasion. *PLoS One*, **8**, e74659.
145. Hoshiba, T. *et al.* (2010) Decellularized matrices for tissue engineering. *Expert Opin. Biol. Ther.*, **10**, 1717–1728.
146. Chuang, H.N. *et al.* (2013) Coculture system with an organotypic brain slice and 3D spheroid of carcinoma cells. *J. Vis. Exp.*, **80**, e50881.
147. Biankin, A.V. *et al.*; Australian Pancreatic Cancer Genome Initiative. (2012) Pancreatic cancer genomes reveal aberrations in axon guidance pathway genes. *Nature*, **491**, 399–405.
148. Morin, K.T. *et al.* (2013) *In vitro* models of angiogenesis and vasculogenesis in fibrin gel. *Exp. Cell Res.*, **319**, 2409–2417.
149. Geudens, I. *et al.* (2011) Coordinating cell behaviour during blood vessel formation. *Development*, **138**, 4569–4583.
150. Zheng, Y. *et al.* (2012) *In vitro* microvessels for the study of angiogenesis and thrombosis. *Proc. Natl Acad. Sci. USA*, **109**, 9342–9347.
151. Yeon, J.H. *et al.* (2012) *In vitro* formation and characterization of a perfusable three-dimensional tubular capillary network in microfluidic devices. *Lab Chip*, **12**, 2815–2822.
152. Chan, J.M. *et al.* (2012) Engineering of *in vitro* 3D capillary beds by self-directed angiogenic sprouting. *PLoS One*, **7**, e50582.
153. Song, J.W. *et al.* (2012) Anastomosis of endothelial sprouts forms new vessels in a tissue analogue of angiogenesis. *Integr. Biol. (Camb.)*, **4**, 857–862.
154. Kim, S. *et al.* (2013) Engineering of functional, perfusable 3D microvascular networks on a chip. *Lab Chip*, **13**, 1489–1500.
155. Friedrich, J. *et al.* (2007) Experimental anti-tumor therapy in 3-D: spheroids—old hat or new challenge? *Int. J. Radiat. Biol.*, **83**, 849–871.
156. Truong, H.H. *et al.* (2012) Automated microinjection of cell-polymer suspensions in 3D ECM scaffolds for high-throughput quantitative cancer invasion screens. *Biomaterials*, **33**, 181–188.
157. Yuhas, J.M. *et al.* (1977) A simplified method for production and growth of multicellular tumor spheroids. *Cancer Res.*, **37**, 3639–3643.
158. Ijima, H. *et al.* (2009) Primary rat hepatocytes form spheroids on hepatocyte growth factor/heparin-immobilized collagen film and maintain high albumin production. *Biochem. Engineer. J.*, **46**, 227–233.
159. Foty, R. (2011) A simple hanging drop cell culture protocol for generation of 3D spheroids. *J. Vis. Exp.*, **51**, e2720.
160. Bakker, G.J. *et al.* (2012) Fluorescence lifetime microscopy of tumor cell invasion, drug delivery, and cytotoxicity. *Methods Enzymol.*, **504**, 109–125.
161. Throm, A.M. *et al.* (2010) Development of a cell-derived matrix: effects of epidermal growth factor in chemically defined culture. *J. Biomed. Mater. Res. A*, **92**, 533–541.
162. Hughes, C.S. *et al.* (2010) Matrigel: a complex protein mixture required for optimal growth of cell culture. *Proteomics*, **10**, 1886–1890.
163. Astashkina, A. *et al.* (2012) A critical evaluation of *in vitro* cell culture models for high-throughput drug screening and toxicity. *Pharmacol. Ther.*, **134**, 82–106.
164. Kleinman, H.K. *et al.* (2005) Matrigel: basement membrane matrix with biological activity. *Semin. Cancer Biol.*, **15**, 378–386.
165. Francis, D. *et al.* (2009) Myogel supports the ex-vivo amplification of corneal epithelial cells. *Exp. Eye Res.*, **88**, 339–346.
166. Abberton, K.M. *et al.* (2008) Myogel, a novel, basement membrane-rich, extracellular matrix derived from skeletal muscle, is highly adipogenic *in vivo* and *in vitro*. *Cells. Tissues. Organs*, **188**, 347–358.
167. Fusenig, N.E. *et al.* (1983) Growth and differentiation characteristics of transformed keratinocytes from mouse and human skin *in vitro* and *in vivo*. *J. Invest. Dermatol.*, **81**(suppl. 1), 168s–175s.
168. Wu, J. *et al.* (2012) Optical imaging techniques in microfluidics and their applications. *Lab Chip*, **12**, 3566–3575.
169. Huang, Y. *et al.* (2011) Microfluidics-based devices: New tools for studying cancer and cancer stem cell migration. *Biomicrofluidics*, **5**, 13412.
170. Song, H. *et al.* (2010) An integrated microfluidic cell array for apoptosis and proliferation analysis induction of breast cancer cells. *Biomicrofluidics*, **4**, 44104.

Received November 21, 2013; revised April 29, 2014;  
accepted May 5, 2014